Diode-pumped mode-locked femtosecond Tm:CLNGG disordered crystal laser

J. Ma,[1] G. Q. Xie,[1,*] W. L. Gao,[1] P. Yuan,[1] L. J. Qian,[1] H. H. Yu,[2] H. J. Zhang,[2] and J. Y. Wang[2]

[1]*Department of Physics, Key Laboratory for Laser Plasmas (Ministry of Education), State Key Lab of Advanced Optical Communication Systems and Networks, Shanghai Jiao Tong University, Shanghai 200240, China*

[2]*State Key Laboratory of Crystal Materials and Institute of Crystal Materials, Shandong University, Jinan 250100, China*

**Corresponding author: xiegq@sjtu.edu.cn*

Received December 12, 2011; revised January 28, 2012; accepted February 8, 2012;
posted February 10, 2012 (Doc. ID 159815); published April 12, 2012

A diode-end-pumped passively mode-locked femtosecond Tm-doped calcium lithium niobium gallium garnet (Tm:CLNGG) disordered crystal laser was demonstrated for the first time to our knowledge. With a 790 nm laser diode pumping, stable CW mode-locking operation was obtained by using a semiconductor saturable absorber mirror. The disordered crystal laser generated mode-locked pulses as short as 479 fs, with an average output power of 288 mW, and repetition rate of 99 MHz in 2 μm spectral region.

OCIS codes: 140.3480, 140.3580, 140.4050, 140.3380.

The Tm^{3+} ($^3F_4 \rightarrow {}^3H_6$) or Ho^{3+} ($^5I_7 \rightarrow {}^5I_8$) doped and $Tm^{3+}-Ho^{3+}$ co-doped laser materials attract much interest for CW and pulsed laser operation in the wavelength region around 2 μm, which corresponds to the eye-safe region of the spectrum. Lasers in this spectral region have great potential applications in laser lidar, gas sensing, semiconductor material processing, molecular spectroscopy, medicine, and nonlinear frequency conversion, etc. [1–4]. Since the first experiment on Tm^{3+} and Ho^{3+} doped laser was reported in the 1960s [5], various kinds of 2 μm solid-state lasers with high output powers and high slope efficiencies have been demonstrated in CW regime [6–8]. However, it is not easy to realize mode-locking operation for Tm^{3+} and Ho^{3+} doped bulk lasers because the stimulated emission cross-sections of Tm^{3+} and Ho^{3+} doped materials are usually very small, which causes high CW mode-locking threshold for these lasers [9]. On the other hand, water vapor in atmosphere has a significant absorption for laser radiation at 2 μm wavelength. So far, only a few mode-locked solid-state or fiber lasers have been reported in this spectral region [10–18]. In contrast to Ho^{3+} doped materials, Tm^{3+} doped materials have a great advantage as they could be directly pumped by commercial 790 nm AlGaAs laser diodes. In addition, Tm^{3+} doped laser materials usually have a wide emission spectrum. However, the non-smooth fluorescence spectral shape with spike structures limits the generated pulse duration from Tm^{3+} ion mode-locked lasers.

In recent years, disordered crystal has been verified to be a kind of excellent ultrafast laser medium. In disordered crystals, some cation ions could randomly distribute in some lattice sites, which causes considerable inhomogeneous spectrum line broadening and splitting. Thus, the disordered crystal laser could generate much shorter mode-locked pulses. Calcium lithium niobium gallium garnet (CLNGG) is a typical disordered crystal. In CLNGG disordered crystal, the Nb^{5+} and Ga^{3+} has a random distribution in some lattice sites, which causes disordered crystal lattice field and inhomogeneous spectrum line broadening. A passively mode-locked Nd-doped CLNGG disordered crystal laser has been reported, which generated much shorter pulses compared with other Nd-doped single crystal lasers at 1 μm wavelength [19]. Recently, the wavelength tuning characteristic of the CW Tm:CLNGG laser was investigated and a wide tuning range from 1896 to 2069 nm was obtained [20]. The wide tuning range of Tm:CLNGG implies the potential for generation of ultrashort mode-locked pulses at 2 μm wavelength.

Up to now, Tm^{3+} doped mode-locked bulk lasers are usually pumped by Ti:sapphire lasers due to their good beam quality and high brightness. Pulses as short as 386 fs, 410 fs, and 10 ps were generated from Tm:$KY(WO_4)_2$ crystal [15], Tm:GPNG fluorogermanate glass [11], and Tm:$KLu(WO_4)_2$ crystal [21] lasers pumped by CW Ti:sapphire laser. However, the high cost and bulky volume of the Ti:sapphire laser system would limit the applications of these 2 μm lasers. By comparison, with commercial laser diode pumping, only a Tm:$GdLiF_4$ mode-locked laser [10] has been reported, which generated 17 ps pulses with an average output power of 38 mW.

In this Letter, we report on a passively mode-locked Tm:CLNGG disordered crystal laser pumped by an AlGaAs laser diode at 790 nm. With a semiconductor saturable absorber mirror (SESAM) as mode-locker, the disordered crystal laser generated stable mode-locked pulses with pulse duration as short as 479 fs, repetition rate of 99 MHz, and average output power of 288 mW. To the best of our knowledge, this is the first demonstration of femtosecond mode-locked bulk laser in the 2 μm spectral region directly pumped by a commercial laser diode.

The schematic of the mode-locked laser setup is shown in Fig. 1. A single-emitter AlGaAs laser diode at 790 nm (nLight Laser, NL-C-5.0-790-3-F) was used as the pump source. The pump light was focused into the Tm:CLNGG crystal by two coupling convex lenses with the same focal length of 100 mm. The focused pump spot radii were measured to be about 25 μm (horizontal direction) × 86 μm (vertical direction) in the air, with corresponding Rayleigh lengths of ~5 mm × 3 mm in two directions. The Tm:CLNGG crystal employed in the experiment was grown by Czochralski technique with Tm^{3+} concentration of 3 at. % in melt. The sample had a size of 9 mm in length and 4 mm × 4 mm in cross-section, and both end faces were Brewster cut and optically polished to

0146-9592/12/081376-03$15.00/0

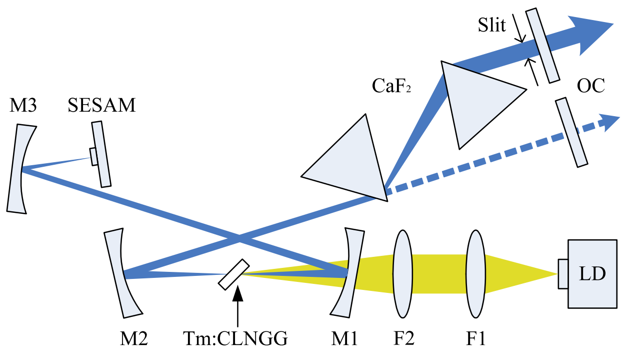

Fig. 1. (Color online) Schematic of the passively mode-locked Tm:CLNGG laser. F1, F2: convex lens, $f = 100$ mm. M1, M2 and M3: plano-concave highly reflective mirrors, radius of curvature (ROC) = −100 mm. OC: output coupler.

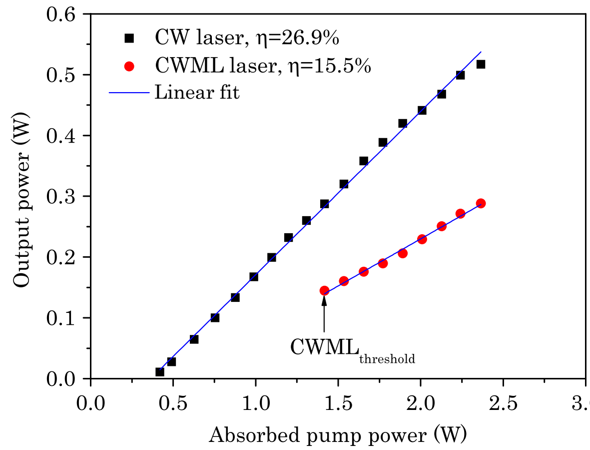

Fig. 2. (Color online) Output power versus absorbed pump power in different operation regimes.

minimize transmission losses for p polarization. To remove the generated heat while pumping, the crystal was wrapped with indium foil and tightly mounted in a water-cooled copper block, and the circulating water temperature was sustained at 9.0 °C. An X-folded five mirrors cavity was used in the experiment to achieve suitable laser mode sizes in the laser crystal and on the SESAM. Based on the ABCD propagation matrix method, the laser mode size was calculated to be about $35\ \mu\text{m} \times 35\ \mu\text{m}$ in radius. The three folding mirrors M1, M2, and M3 have the same radius of curvature of 100 mm, and were all highly reflectively coated for laser wavelength and anti-reflectively coated for pumping wavelength (transmission $> 95\%$ at 790 nm, reflectivity $> 99.7\%$ from 1850 to 2100 nm). The wedged plano-plano output coupler has a transmission of 2% from 1850 to 2100 nm. The SESAM (BATOP GmBH) was designed to operate at 2000 nm with a modulation depth of 3%, a relaxation time of 5 ps, and a saturation fluence of 60 $\mu\text{J/cm}^2$. A pair of CaF_2 prisms with a tip-to-tip distance of 39 cm was used to compensate the cavity dispersion of the resonator.

The negative dispersion provided by the prism pair was calculated to be about $-963\ \text{fs}^2$. In addition, a slit was placed close to the output coupler to suppress the high-order transverse mode oscillation in the vertical direction.

Firstly, the CW operation performance of the laser was investigated while no prisms were inserted in the cavity and the SESAM was replaced by a highly-reflective plane mirror. The laser output power was measured with a thermo-sensitive power meter (THORLABS, PM320E). As shown in Fig. 2, the maximum output power of 517 mW was obtained under an absorbed pump power of 2.36 W, with a slope efficiency of 26.9%. Due to a low absorption coefficient ($\sim 0.94\ \text{cm}^{-1}$) of the employed Tm:CLNGG, a long crystal of 9 mm was used in the experiment to efficiently absorb the pump light. However, the Rayleigh length of the pump light in the slow axis direction was only ~3 mm, thus resulting in a poor mode matching between pumping spot and laser mode. The low slope efficiency could be attributed to the poor mode matching.

When the SESAM was employed and the prism pair was plugged in the cavity, stable CW mode-locking of the laser could be achieved. As the incident pump power increased, the laser operation changed from CW to Q-switched mode-locking and finally to stable CW mode-locking. However, in the Q-switched mode-locking regime, SESAM could be easily damaged by Q-switched mode-locked pulses, accompanying with a remarkable decrease of average output power of the laser. In the experiment, once CW mode-locking was established, it could be sustained for several hours. The mode-locked pulse trains were measured with a high speed detector (EOT, ET-5000) and displayed on a digital oscillator with 500 MHz bandwidth (Tektronix, DPO3054). Figure 3 shows the typical mode-locked pulse trains in nanosecond and millisecond time scales. The pulse repetition rate was 99 MHz, corresponding to the laser cavity length of 1.51 m. The average output power in CW mode-locking operation of the laser as a function of absorbed pump power is shown in Fig. 2 (red dot). The CW mode-locking threshold was about 1.42 W of absorbed pump power, below which the SESAM was easily damaged due to Q-switched mode-locking. The maximum average output power was 288 mW with an absorbed pump power of 2.36 W, and higher output power was limited only by the available pump power. Comparing with CW operation, the lower slope efficiency of 15.5% in CW mode-locking operation could be attributed to the large nonsaturable absorption (2%) of the SESAM.

The autocorrelation trace and optical spectrum of the mode-locked pulses are shown in Fig. 4. The autocorre-

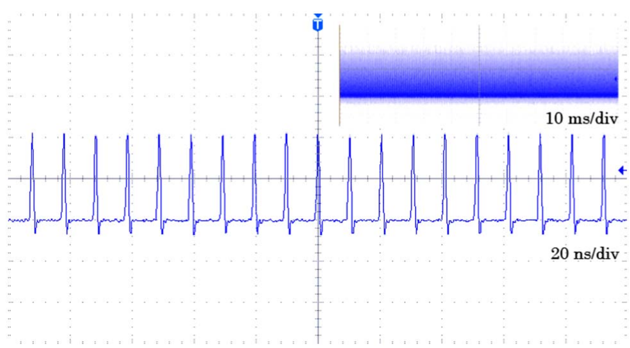

Fig. 3. (Color online) CW mode-locked pulse trains in nanosecond and millisecond time scales.

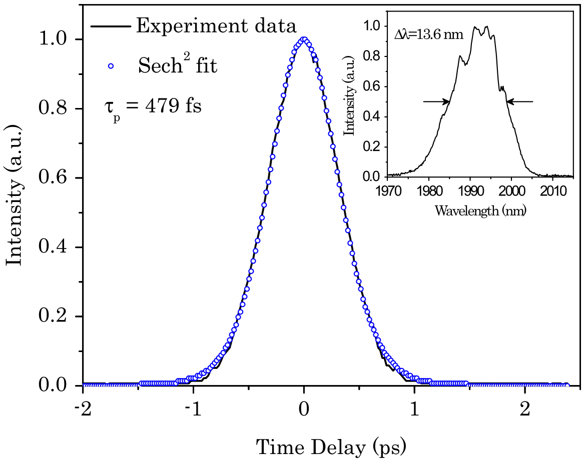

Fig. 4. (Color online) Autocorrelation trace and optical spectrum (inset) of the mode-locked pulses.

lation trace obtained from a commercial autocorrelator (APE, Pulse Check 50) is well fitted assuming a sech^2-pulse shape, the mode-locked pulse duration was 479 fs. In the experiment, we attempted to optimize intracavity dispersion by changing the inserting thickness of the prisms, but no shorter pulses have been obtained. The mode-locked pulse spectrum was measured by a mid-infrared (mid-IR) optical spectrum analyzer with a resolution of 0.22 nm. The spectrum is centered at 1994 nm with a FWHM bandwidth of 13.6 nm. The time–bandwidth product is calculated to be 0.49, which is 1.6 times of the Fourier transform limit value for the sech^2-shape pulses. According to [22], we believe that the mode-locked pulses could be further shortened by employing SESAM with shorter relaxation time and less nonsaturable absorption.

In conclusion, we have experimentally demonstrated a diode-pumped passively mode-locked femtosecond Tm:CLNGG disordered crystal laser at 2 μm wavelength for the first time to our knowledge. The disordered crystal laser generated mode-locked pulses with a pulse duration as short as 479 fs, a repetition rate of 99 MHz, and an average output power of 288 mW at 1994 nm wavelength. The diode-pumped compact femtosecond mid-IR laser would have potential applications in ultrafast molecule spectroscopy, mid-IR nonlinear frequency conversion, etc.

The work is partially supported by National Natural Science Foundation of China (nos. 61008018, 60890202, and 61008017).

References

1. S. W. Henderson, C. P. Hale, J. R. Magee, M. J. Kavaya, and A. V. Huffaker, Opt. Lett. **16**, 773 (1991).
2. P. A. Budni, L. A. Pomeranz, M. L. Lemons, C. A. Miller, J. R. Mosto, and E. P. Chicklis, J. Opt. Soc. Am. B **17**, 723 (2000).
3. T. Fuji, N. Ishii, C. Y. Teisset, X. Gu, T. Metzger, A. Baltuska, N. Forget, D. Kaplan, A. Galvanauskas, and F. Krausz, Opt. Lett. **31**, 1103 (2006).
4. B. Walsh, Laser Phys. **19**, 855 (2009).
5. L. F. Johnson, J. Appl. Phys. **34**, 897 (1963).
6. E. C. Honea, R. J. Beach, S. B. Sutton, J. A. Speth, S. C. Mitchell, J. A. Skidmore, M. A. Emanuel, and S. A. Payne, IEEE J. Quantum Electron. **33**, 1592 (1997).
7. P. Koopmann, S. Lamrini, K. Scholle, P. Fuhrberg, K. Petermann, and G. Huber, Opt. Lett. **36**, 948 (2011).
8. M. Schellhorn, S. Ngcobo, and C. Bollig, Appl. Phys. B **94**, 195 (2009).
9. C. Hönninger, R. Paschotta, F. Morier-Genoud, M. Moser, and U. Keller, J. Opt. Soc. Am. B **16**, 46 (1999).
10. N. Coluccelli, G. Galzerano, D. Gatti, A. Di Lieto, M. Tonelli, and P. Laporta, Appl. Phys. B **101**, 75 (2010).
11. F. Fusari, A. A. Lagatsky, G. Jose, S. Calvez, A. Jha, M. D. Dawson, J. A. Gupta, W. Sibbett, and C. T. A. Brown, Opt. Express **18**, 22090 (2010).
12. A. A. Lagatsky, F. Fusari, S. Calvez, S. V. Kurilchik, V. E. Kisel, N. V. Kuleshov, M. D. Dawson, C. T. A. Brown, and W. Sibbett, Opt. Lett. **35**, 172 (2010).
13. A. A. Lagatsky, X. Han, M. D. Serrano, C. Cascales, C. Zaldo, S. Calvez, M. D. Dawson, J. A. Gupta, C. T. A. Brown, and W. Sibbett, Opt. Lett. **35**, 3027 (2010).
14. N. Coluccelli, A. Lagatsky, A. D. Lieto, M. Tonelli, G. Galzerano, W. Sibbett, and P. Laporta, Opt. Lett. **36**, 3209 (2011).
15. A. A. Lagatsky, S. Calvez, J. A. Gupta, V. E. Kisel, N. V. Kuleshov, C. T. A. Brown, M. D. Dawson, and W. Sibbett, Opt. Express **19**, 9995 (2011).
16. A. Härkönen, C. Grebing, J. Paajaste, R. Koskinen, J.-P. Alanko, S. Suomalainen, G. Steinmeyer, and M. Guina, Electron. Lett. **47**, 454 (2011).
17. R. C. Sharp, D. E. Spock, N. Pan, and J. Elliot, Opt. Lett. **21**, 881 (1996).
18. G. Imeshev and M. E. Fermann, Opt. Express **13**, 7424 (2005).
19. G. Q. Xie, D. Y. Tang, W. D. Tan, H. Luo, H. J. Zhang, H. H. Yu, and J. Y. Wang, Opt. Lett. **34**, 103 (2009).
20. W. L. Gao, G. Q. Xie, J. Ma, M. N. Liu, P. Yuan, L. J. Qian, H. H. Yu, H. J. Zhang, J. Y. Wang, and J. Zhang, "Spectroscopic characteristics and efficient laser operation of Tm:CLNGG disordered crystal," Laser Phys. Lett. (to be published).
21. W. B. Cho, A. Schmidt, J. H. Yim, S. Y. Choi, S. Lee, F. Rotermund, U. Griebner, G. Steinmeyer, V. Petrov, X. Mateos, M. C. Pujol, J. J. Carvajal, M. Aguiló, and F. Díaz, Opt. Express **17**, 11007 (2009).
22. R. Paschotta and U. Keller, Appl. Phys. B **73**, 653 (2001).